



In silico study the inhibition of angiotensin converting enzyme 2 receptor of COVID-19 by *Ammoides verticillata* components harvested from Western Algeria

Imane Abdelli^{a,b}, Faiçal Hassani^c, Sohayb Bekkel Brikci^c and Said Ghalem^b

^aHigher School of Applied Sciences, Tlemcen, Algeria; ^bLaboratory of Natural and bio-actives Substances, Faculty of Science- University, Tlemcen, Algeria; ^cEcology and Management of Naturals Ecosystems Laboratory, Department of Ecology and Environment, Faculty SNV-STU- University, Tlemcen, Algeria

Communicated by Ramaswamy H. Sarma

ABSTRACT

The objective of this present study is to focus on the *in silico* study to screen for an alternative drug that can block the activity of the angiotensin converting enzyme 2 (ACE2) as a receptor for SARS-CoV-2, potential therapeutic target of the COVID-19 virus using natural compounds (Isothymol, Thymol, Limonene, P-cymene and γ -terpinene) derived from the essential oil of the antiviral and antimicrobial plant *Ammoides verticillata* (Desf.) Briq. which is located in the occidental Algeria areas. This study reveals that Isothymol, a major component of this plant, gives the best docking scores, compared to, the co-crystallized inhibitor β -D-mannose of the enzyme ACE2, to Captopril drug as good ACE2 inhibitor and to Chloroquine antiviral drug also involved in other mechanisms as inhibition of ACE2 cellular receptor. *In silico* (ADME), drug-likeness, PASS & P450 site of metabolism prediction, pharmacophore Mapper showed that the compound Isothymol has given a good tests results compared to the β -D-mannose co-crystallized inhibitor, to Captopril and Chloroquine drugs. Also the other natural compounds gave good results. The Molecular Dynamics Simulation study showed good result for the Isothymol- ACE2 docked complex. This study revealed for the first time that Isothymol is a functional inhibitor of angiotensin converting enzyme 2 activity and the components of essential oils *Ammoides verticillata* can be used as potential inhibitors to the ACE2 receptor of SARS-CoV-2.

ARTICLE HISTORY

Received 7 April 2020
Accepted 24 April 2020

KEYWORDS

Ammoides verticillata;
Angiotensin converting
enzyme 2; COVID-19;
isothymol; molcular docking

1. Introduction

Coronaviruses are a large virus's family that causes illnesses ranging from a common cold (some seasonal viruses are coronaviruses) to more severe conditions such as SARS-CoV or Mers-CoV (Jabeer Khan et al., 2020; Enayatkhani et al., 2020; Elfiky & Azzam, 2020). This virus is from the family Coronaviridae and was detected in the city of Wuhan in China (Khan et al., 2020; Elmezayen et al., 2020). It was originally named 2019-nCoV. It is now called SARS-CoV-2 (Pant et al., 2020). The disease associated with this virus is COVID-19. The onset of the COVID-19 atypical pneumonia outbreak was reported on December 31, 2019 (Sarma et al., 2020; Gupta et al., 2020). Common symptoms include fever, cough, and shortness of breath. Other symptoms may include fatigue, muscle pain, diarrhea, sore throat, loss of smell, and abdominal pain (Hopkins, 2020). The time from exposure to onset of symptoms is typically around five days but may range from two to fourteen days (Velavan & Meyer, 2020). While the majority of cases result in mild symptoms, some progress to viral pneumonia and multi-organ failure (Hui et al., 2020; Muralidharan et al., 2020). As of 16 April 2020, more than 2.13 million cases have been reported across 210 countries and territories, resulting in more than 142,000 deaths. More than 540,000 people have recovered.

Coronaviruses have in common proteins designated by a letter indicating their location: S (protuberances), E (envelope), M (membrane) and N (nucleocapsid). Some, in particular those of subgroup A of the genus Betacoronavirus, have a characteristic HE protein (hemagglutinin esterase). The SARS coronavirus also presents on protein S a specific binding site for the angiotensin converting enzyme 2 (ACE2) which serves as an entry point into the host cell (Fang, 2005). Research suggests that the receptor is another potential target for vaccines or therapies. An inhibitor that blocks the receptor could make it more difficult for coronavirus to enter cells, which could at least significantly slow the epidemic until the virus disappears (Boopathy et al., 2020; Hasan et al., 2020).

Hence the interest of our study which consists in studying *in silico* the inhibition of ACE 2 by molecules derived from the essential oil of a medicinal plant which bears the name *Ammoides verticillata* (Desf.) Briq. This plant, is an aromatic plant widely used in western Algeria for its culinary and therapeutic purposes, it has proven antioxidant and antimicrobial activities of essential oil (Bekhechia et al., 2010). The different names of *Ammoides verticillata* (Desf.) Briq. are French name Ajowan (Bekhechia et al., 2010), Arabic name Nounkha Taleb El Koubs (Narayana et al., 1967), Nûnkha (Trabut, 1935a; Abdelouahid & Bekhechi, 2002). According to

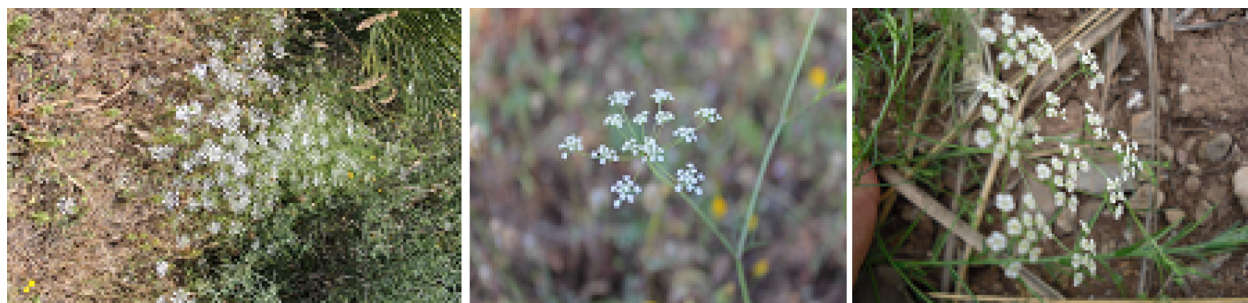


Figure 1. *Ammoides verticillata* (Desf.) Briq from western Algeria.

(Quezel & Santa, 1963), this species is an annual herb that grows spontaneously in the matorrals of the western region of Algeria. This thread-like Apiaceae, with branched stems of 10–40 cm, without rosette of basal leaves. Lower petiolate leaves have many whorled multifid segments, upper pinnatifid leaves have linear segments. The main umbels are 8 - 15 rays. Ovoid fruit is less than 1 mm long Figure 1. It is generally found in fields, lawns, mountains and forests.

Studies have shown that the essential oil of *Ammoides verticillata* has very good antimicrobial activity against five bacterial strains (*Bacillus cereus*, *Staphylococcus aureus*, *Escherichia coli*, *Listeria monocytogenes* and *Micrococcus luteus*) and the yeast *Candida albicans*, with CIM values between 0.78 and 2.34 $\mu\text{l/ml}$. In addition, the essential oil can trap 50% of the free DPPH radical at a concentration of 15.37 $\mu\text{g/ml}$ (Sandberg & Corrigan, 2001; Higley & Higley, 2005; Pole, 2013). Also other study show that aerial parts (leaves and flowers) of *Ammoides verticillata* (Desf.) Briq. collected in occidental Algeria areas, exhibited a very unusual composition. Isothymol was by far the major component (51.2%), accompanied by p-cymene (14.1%), thymol (13.0%), limonene (11.9%) and γ -terpinene (6.8%) (Kambouche & El-Abed, 2003). According to (Lawrence, 2006), it is worth noting that this oil is the richest source of naturally occurring isothymol (Bekhechia et al., 2010). The aims of this study consist to establish a structure–activity relationship of active principles of *Ammoides verticillata* compounds: Isothymol, Thymol, Limonene, P-Cymene and γ -Terpinene against ACE 2 activity compared to β -D- Mannose, co-crystallized inhibitor of this enzyme, this molecule is used in the RCSB data bank to block the ACE2 enzyme activity, and we compared also our results with 2 drugs which are used as good inhibitors to ACE2, the Captopril hypertension drug and Chloroquine anti-malarials and amebicides drug which has also previously shown activity on coronavirus replication (Guastalegname & Vallone, 2020). In this work we will take it as a witness for the discussion of our results to lead to other inhibitors which can also block the ACE2 enzyme activity and used as potential treatment of COVID-19. For this purpose, a molecular docking study was applied for testing the type of interactions between active site residues and the active compounds from *Ammoides verticillata* with ACE2, and calculation of the binding free energies (S-score, kcal/mol) and bonds in order to predict the binding model of the selected compound to the three-dimensional structure of the enzyme (Aanouz et al., 2020).

2. Material and methods

2.1. Ligands and protein preparation

The three-dimensional (3D) structures of compounds Table 1 were pre-optimized by means of the Molecular Mechanics Force Field (MM+). After that, the resulted minimized structures were further refined using the semi-empirical AM1 (Stewart, 2007) with the Polak-Ribiere conjugate gradient algorithm of 0.01 kcal/(Åmol). All methods are implemented in Hyperchem 8.0.8 software (HyperChem v8, 2009), a database was created in which all the ligands were converted into their 3D structures and was used as input MOE-docking.

The X-ray crystal co-ordinates of ACE 2 (PDB ID: 6vw1) (Shang et al., 2020) in the bound state with β -D- Mannose (formula: $\text{C}_6\text{H}_{12}\text{O}_6$) Table 2, were retrieved from RCSB Database (<http://www.rcsb.org/pdb>) Figures 2 and 3. This is selected for modeling studies. In the last, the energy of the proteins structures is minimized using the Energy minimization algorithm of MOE tool. These energy of proteins are calculated (in kcal/mol) by MOE using MMFF94x force field with conjugant gradient method.

2.2. Molecular docking protocol

Docking calculations were carried out using standard default parameter settings in the MOE software package (*Molecular Operating Environment (MOE)*, 2013). In this molecular docking program, the flexibility of ligands is considered while the proteins are considered as a rigid structure. In this case β -D- Mannose is first re-docked into the binding site pocket of ACE2 enzyme, and the root-mean-square deviation (RMSD) values between the docking and initial poses were calculated. In general, the protein structure with a resolution between 1.5 and 2.5 Å have a good quality for further studies (Clément & Slenzka, 2006; Didierjean & Tête-Favier, 2016), whereas, the resolution value of ACE2 not far to this interval. At the end of molecular docking, the best conformations of the ligands were analyzed for their binding interactions and were evaluated by the binding free energies (S-score, kcal/mol) and bonds interactions between ligand atom and active site residues.

2.3. Ligand based druglikeness, ADME/toxicity properties and PASS prediction

Many potential therapeutic agents fail to reach the clinic trials because of their unfavorable absorption, distribution,

Table 1. 2D&3D representations of the all ligands used in the experiment. The ligands structures were taken from PubChem server (www.pubchem.ncbi.nlm.nih.gov).

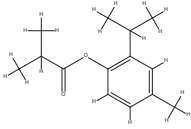
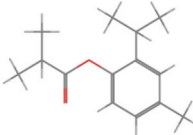
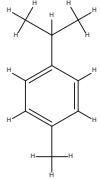
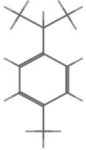
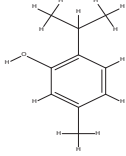
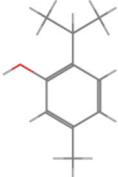
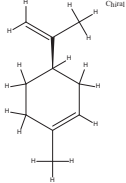
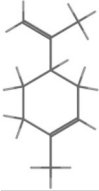
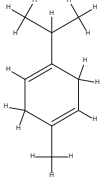
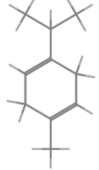
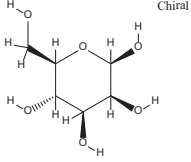
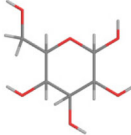
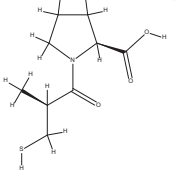
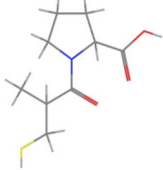
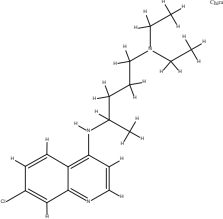
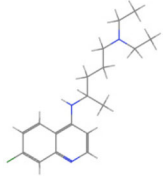
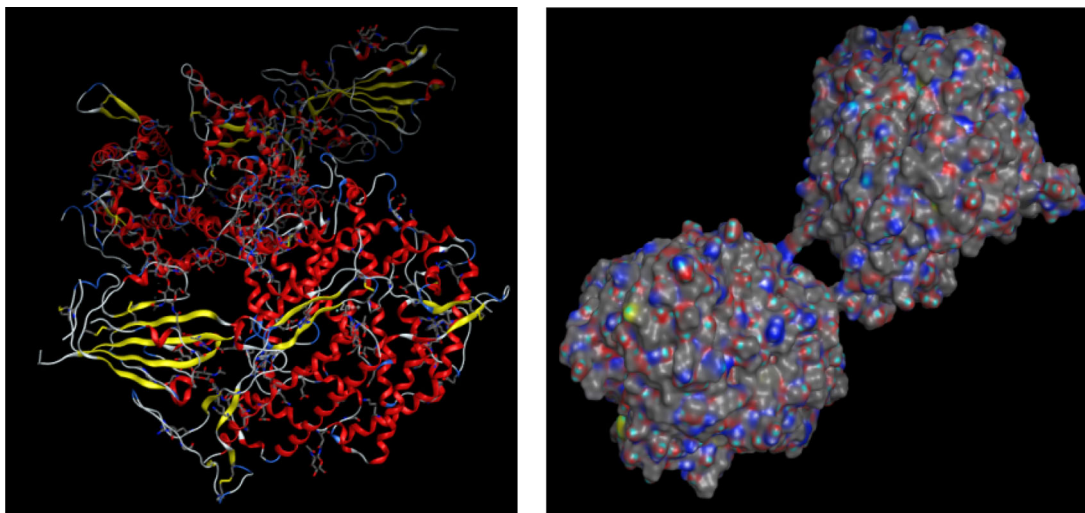
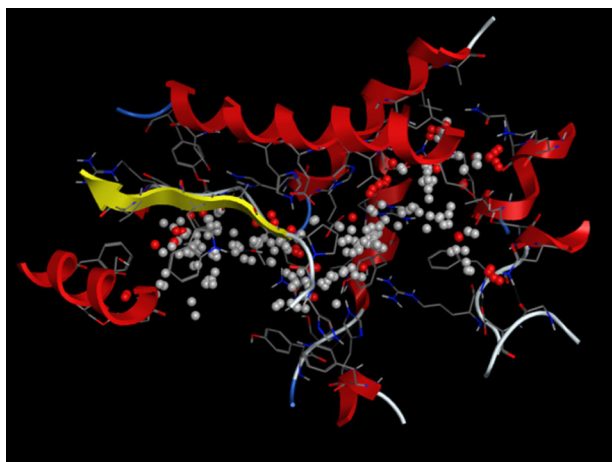
Compound name	2D Structure	3D Structure
Isothymol		
p-cymene		
Thymol		
limonene		
γ -terpinene		
beta-D-Mannose (Co-crystallized ligand)		
Captopril		
Chloroquine		

Table 2. Details related to the ACE2.

Proteins	Methods	Resolution (Å)	R-Value	Residues number	Co-crystallized ligand	Docking Score Kcal/mol
ACE2 PDB ID:6vw1	X-ray diffraction	2.68	0.229	597	β-D-Mannose	-5.4107

**Figure 2.** 3D structure of 2019-nCoV chimeric receptor-binding domain complexed with its receptor human ACE2 enzyme (PDB ID: 6vw1). The structure was taken from Protein Data Bank online server (<https://www.rcsb.org/>) and *Molecular Operating Environment (MOE)*.**Figure 3.** 3D structure of active site enzyme.

metabolism, and elimination (ADME) parameters; also it is not checking the druglikeness. Lipinski's rule of five (Lipinski et al., 2001) Veber's rule (Veber et al., 2002), Egan's rule (Veber et al., 2000) and Polar surface area (TPSA), number of rotatable (Daina et al., 2017), the ADME/Toxicity (pharmacological and pharmacodynamic) properties, the PASS prediction, the P450 Site of Metabolism (SOM) and the Molecular Target studies were calculated using respectively SwissADME properties calculation online, PASS-Way2Drug server, RS-WebPredictor 1.0 and swiss target prediction.

2.4. Pharmacophore mapping

A pharmacophore consists of a pharmacologically active part of a molecule serving as a model. Pharmacophores are therefore sets of active atoms used in the design of drugs. The pharmacophore is an idealized geometric representation,

only 3D modeling can allow optimal use for the creation of new drugs.

A pharmacophore is the set of functional groups arranged in an adequate spatial arrangement, ensuring the fixation of the drug on the receptor and therefore capable of inducing the physiological response.

In this study the Pharmacophore Mapping is carried out for Isothymol the best ligand among the selected ligands using MOE software package (*Molecular Operating Environment (MOE)*, 2013).

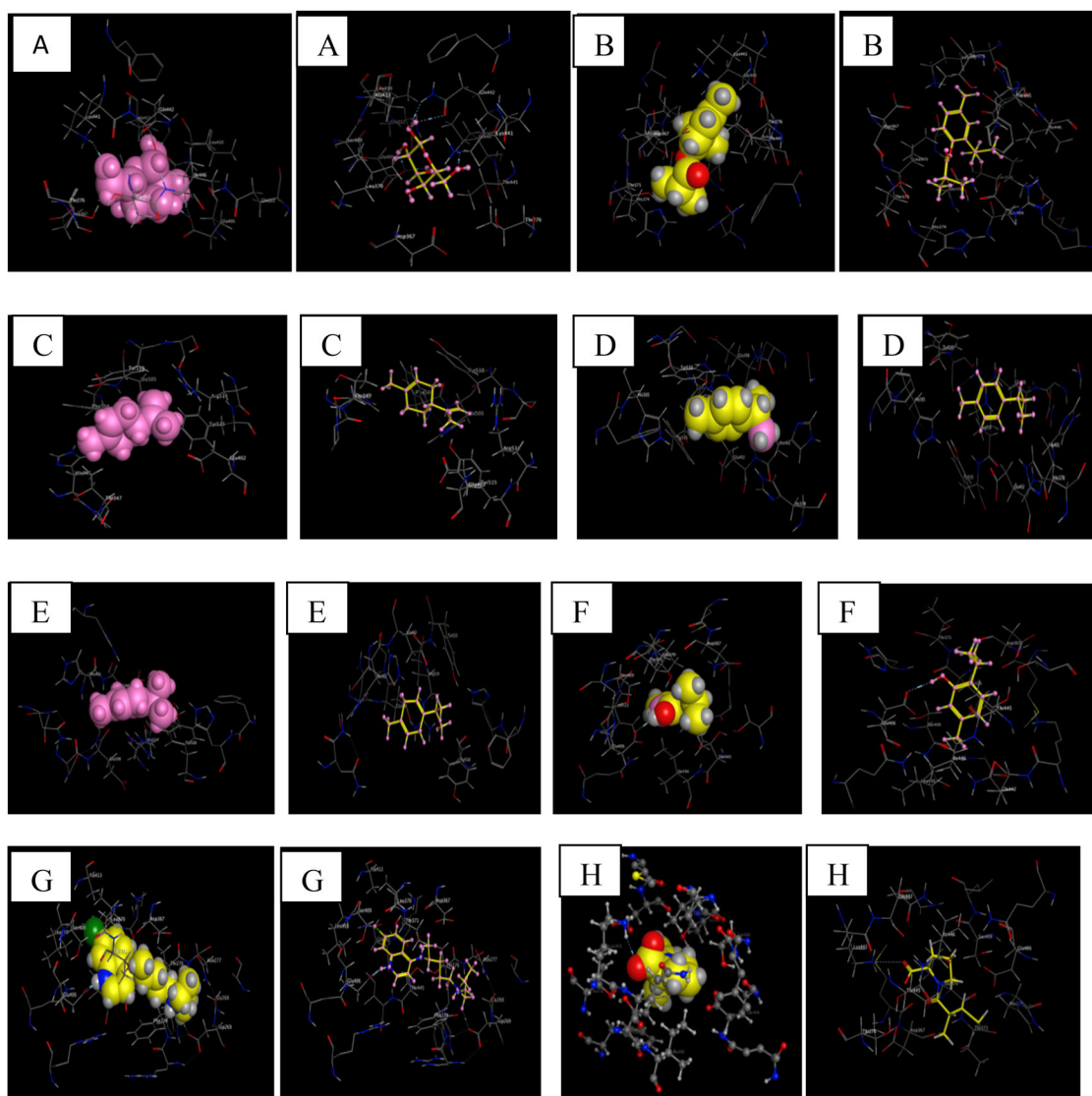
2.5. Molecular dynamics simulation

The molecular dynamics simulation study was carried out for the ligand that was declared as the best among the selected molecules. From the analysis of the results, it was declared that, Isothymol was the best ligand among the selected ligands and molecules. The molecular dynamics simulation study of Isothymol and ACE2 docked complex was performed by iMODS. It is a fast, user-friendly and effective molecular dynamics simulation tool that can be used efficiently to investigate the structural dynamics of the protein complexes. It provides the values of deformability, B-factor (mobility profiles), eigenvalues, variance, co-variance map and elastic network. For a complex or protein, the deformability depends on the ability to deform at each of its amino acid residues. The eigenvalue has relation with the energy that is required to deform the given structure and the lower the eigenvalue, the easier the deformability of the complex.

Moreover, the eigenvalue also represents the motion stiffness of the protein complex. iMODS is a fast and easy server for determining and measuring the protein flexibility (Awan et al., 2017; Prabhakar et al., 2016; López-Blanco et al., 2014; López-Blanco et al., 2011)

Table 3. The docking results (binding energy) of all ligands and the controls along their respective number of hydrogen bonds as well as interacting amino acids.

Names of ligands	SP Docking Score (Binding Energy) (Kcal/mol)	Interacting residues of the target	Types of bonds	Distance (Å)	Energies (kcal-mol)
Chloroquine	-6.4530	OE1-GLU402 OE1-GLU406	H-donor Ionic	3.42 2.86	-1.0 -5.5
Isothymol	-5.7853	6-ring-THR445	Pi-H	4.06	-0.6
beta-D-Mannose (Co-cristallisation ligand)	-5.4107	O3-OE2 GLU 406 O4- OE2 GLU 406 O5-OE1 GLN 442 O5-NE2 GLN 442 O6-NZ LYS 441	H-donor H-donor H-donor H-acceptor H-acceptor	2.99 2.94 2.90 3.08 3.15	-2.5 -1.0 -1.2 0.3 -2.7
Captopril	-5.2248	NZ-LYS 441	Ionic	3.12	-1.0
Thymol	-4.7450	O1-OE1 GLU 406 6-ring- CG2 THR445	H-donor Pi-H	3.17 4.33	-3.0 -0.9
limonene	-4.4067	/	/	/	/
p-cymene	-4.3630	/	/	/	/
γ -terpinene	-4.2320	/	/	/	/

**Figure 4.** 3D representations of the best pose interactions between the ligands and their receptor. A. interaction between β -D-Mannose Co-cristallized ligand) and ACE2, B. interaction between Isothymol and ACE2, C. interaction between limonene and ACE2, D. interaction between p-cymene and ACE2, E. interaction between γ -terpinene and ACE2, F. interaction between Thymol and ACE2, G. interaction between Chloroquine and ACE2, H. interaction between Captopril and ACE2. The 3D representations of the best pose interactions between the ligands and their respective receptors were visualized using *Molecular Operating Environment* (MOE).

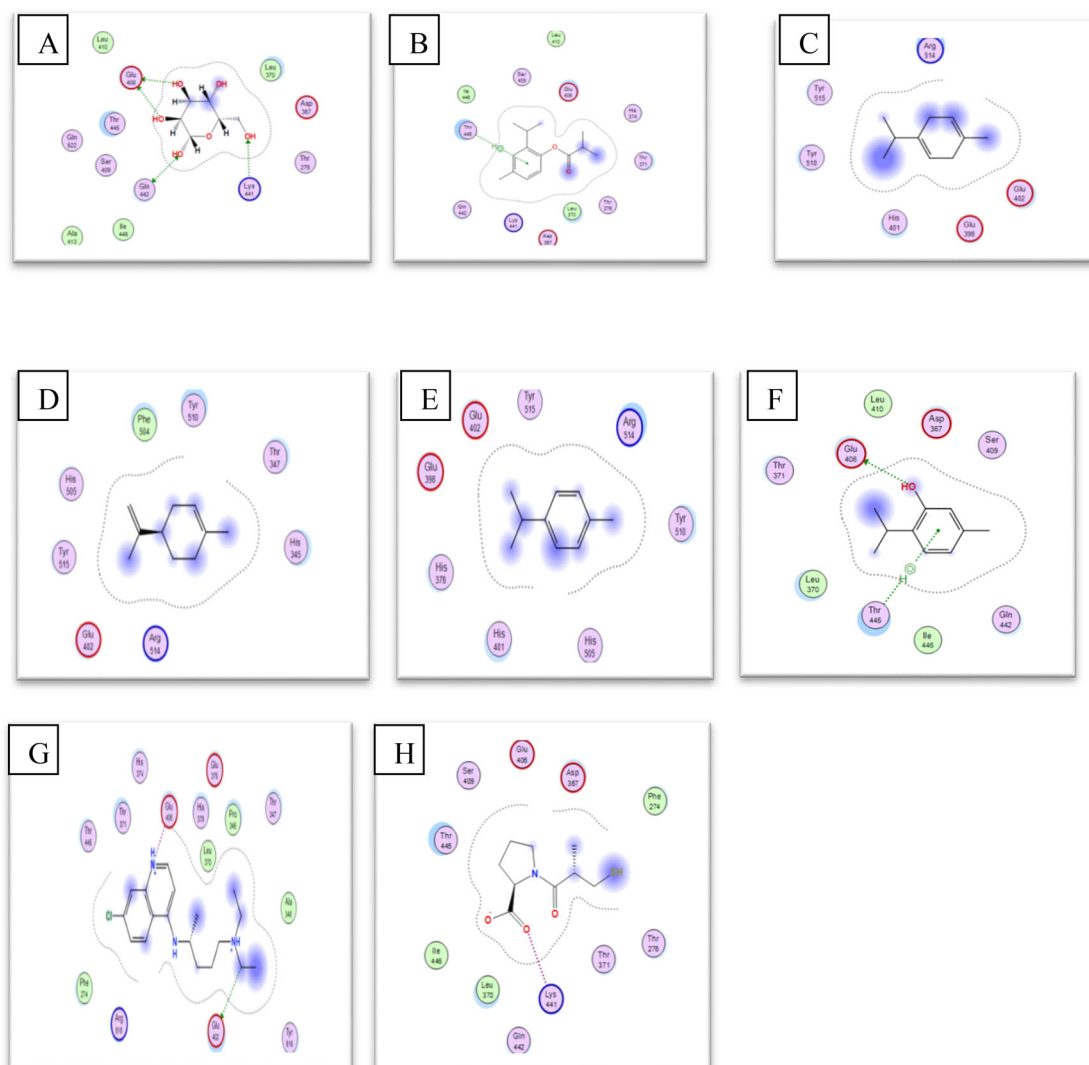


Figure 5. 2D representations of the best pose interactions between the ligands and their receptor. A. interaction between β -D-Mannose (Co-crystallized ligand) and ACE2, B. interaction between Isothymol and ACE2, C. interaction between limonene and ACE2, D. interaction between p-cymene and ACE2, E. interaction between γ -terpinene and ACE2, F. interaction between Thymol and ACE2, G. interaction between Chloroquine and ACE2, H. interaction between Captopril and ACE2. The 2D representations of the best pose interactions between the ligands and their respective receptors were visualized using *Molecular Operating Environment* (MOE).

Table 4. List of the results of the ligands druglikeness properties.

Drug Likeness Properties	Chloroquine	Isothymol	beta-D-Mannose	Captopril	Thymol	limonene	p-cymene	γ -terpinene
Molecular weight g/mol	319.87	220.31	180.16	217.29	150.22	136.23	134.22	136.23
Consensus Log Po/w	4.15	3.85	-2.62	0.62	2.84	3.36	3.19	3.05
Log S	-4.06	-3.56	0.25	-1.71	-2.54	-2.54	-2.83	-2.37
Num. H-bond acceptors	2	2	6	3	1	0	0	0
Num. H-bond donors	1	0	5	1	1	0	0	0
Molar Refractivity	97.41	67.10	35.74	59.97	48.01	47.12	45.99	47.12
Lipinski	Yes	Yes	Yes	Yes	Yes	Yes	Yes	Yes
Ghose	Yes	Yes	No	Yes	No	No	No	No
Veber	Yes	Yes	Yes	Yes	Yes	Yes	Yes	Yes
Egan	Yes	Yes	Yes	Yes	Yes	Yes	Yes	Yes
Muegge	Yes	Yes	No	Yes	No	No	No	No
Bioavailability score	0.55	0.55	0.55	0.56	0.55	0.55	0.55	0.55
Synthetic accessibility (SA)	2.76	1.96	4.08	2.47	1.00	3.46	1.00	3.11
TPSA (\AA^2)	28.16	26.30	110.38	96.41	20.23	0.00	0.00 \AA^2	0.00
No of rotatable bonds	8	4	1	4	1	1	1	1
Druglikeness score	7.39	-1.37	-3.78	-0.96	-3.02	-21.85	-5.63	-2.82
Drug-Score	0.30	0.31	0.51	0.63	0.18	0.06	0.22	0.29
Solubility	-4.06	-3.56	0.25	-1.71	-2.54	-2.54	-2.83	-2.37
Reproductive effective irritant	Yes	Yes	Yes	Yes	No	No	Yes	Yes
Tumorigenic	No	No	Yes	Yes	Yes	No	No	No
Mutagenic	Yes	Yes	Yes	Yes	Yes	No	No	Yes
Mutagenic	No	Yes	Yes	Yes	No	No	Yes	Yes

Table 5. The ADME/T test results of ligands (various pharmacokinetic and pharmacodynamic properties).

Class	Properties	Chloroquine	Isothymol	D-Mannose	Captopril	Thymol	limonene	p-cymene	γ -terpinene
Absorption	Caco-2 permeability	Optimal	Optimal	Low	Optimal	Optimal	Optimal	Optimal	Optimal
	Pgp-inhibitor	Non-inhibitor	Inhibitor	Non-inhibitor	Non-inhibitor	Non-inhibitor	Non-inhibitor	Non-inhibitor	Non-inhibitor
Distribution	Pgp-substrate	substrate	Non-substrate	Non-substrate	Non-substrate	Non-substrate	Non-substrate	Non-substrate	Non-substrate
	Human Intestinal Absorption (HIA)	HIA positive	HIA positive	HIA negative	HIA positive	HIA positive	HIA positive	HIA positive	HIA positive
Metabolism	Plasma Protein Binding	Good	Good	Low	Low	Good	Good	Low	Low
	BBB (Blood-Brain Barrier)	BBB positive	BBB positive	BBB positive	BBB negative	BBB positive	BBB positive	BBB positive	BBB positive
	CYP450 1A2 inhibitor	Non-inhibitor	Inhibitor	Non-inhibitor	Non-inhibitor	Inhibitor	Non-inhibitor	Non-inhibitor	Non-inhibitor
	CYP450 1A2 substrate	Substrate	Substrate	Non-substrate	Non-substrate	Substrate	Substrate	Substrate	Substrate
	CYP450 3A4 inhibitor	Non-inhibitor	Non-inhibitor	Non-inhibitor	Non-inhibitor	Non-inhibitor	Non-inhibitor	Non-inhibitor	Non-inhibitor
	CYP450 3A4 substrate	Substrate	Substrate	Non-substrate	Non-substrate	Non-substrate	Non-substrate	Non-substrate	Non-substrate
	CYP450 2C9 inhibitor	Non-inhibitor	Inhibitor	Non-inhibitor	Non-inhibitor	Non-inhibitor	Non-inhibitor	Non-inhibitor	Non-inhibitor
	CYP450 2C9 substrate	Non-substrate	Inhibitor	Non-inhibitor	Non-inhibitor	Non-inhibitor	Non-inhibitor	Non-inhibitor	Non-inhibitor
	CYP450 2C19 inhibitor	Non-inhibitor	Inhibitor	Non-inhibitor	Non-inhibitor	Inhibitor	Non-inhibitor	Non-inhibitor	Non-inhibitor
	CYP450 2C19 substrate	Substrate	Substrate	Non-substrate	Non-substrate	Substrate	Substrate	Substrate	Substrate
Excretion Toxicity	CYP450 2D6 inhibitor	Inhibitor	Non-inhibitor	Non-inhibitor	Non-inhibitor	Non-inhibitor	Non-inhibitor	Non-inhibitor	Non-inhibitor
	CYP450 2D6 substrate	Substrate	Substrate	Non-substrate	Substrate	Substrate	Substrate	Substrate	Substrate
Excretion Toxicity	T1/2 (h)	2.23	1.225	1.129	0.793	1.313	1.741	1.772	1.78
	hERG (hERG Blockers)	Blockers	Non-blockers	Non-blockers	Non-blockers	Non-blockers	Non-blockers	Non-blockers	Non-blockers
	H-HT (Human Hepatotoxicity)	HHT positive	HHT negative	HHT positive	HHT positive	H-HT negative	H-HT negative	HHT negative	H-HT negative
	Ames (Ames Mutagenicity)	Ames positive	Ames negative	Ames	Ames negative	Ames negative	Ames negative	Ames negative	Ames negative
	DILI (Drug Induced Liver Injury)	DILI negative	DILI negative	DILI negative	DILI negative	DILI negative	DILI negative	DILI negative	DILI negative

3. Results and discussion

3.1. Molecular docking simulation

3.1.1. The binding affinities of the ligands into ACE2 active site

The results calculations docking details received after dock all ligands with ACE2 target are listed in the Table 3.

The molecules that had the lowest binding energy of docking score were considered the best molecule and inhibiting the target receptor as the lower binding energy corresponds to higher binding affinity (Simon et al., 2017).

The ACE2-ligands complexes formed are shown in Figure 4.

The binding mode observed for all ligands with pocket of receptor is represented in the Figure 5.

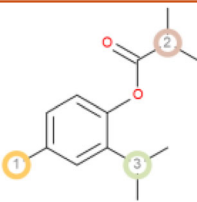
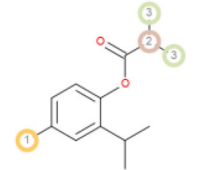
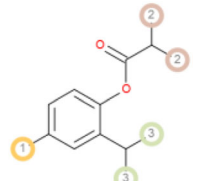
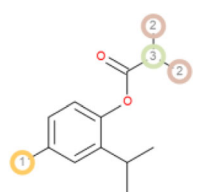
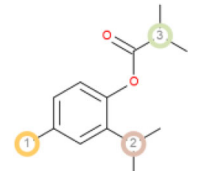
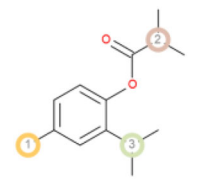
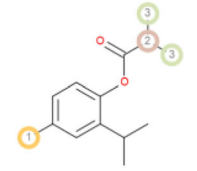
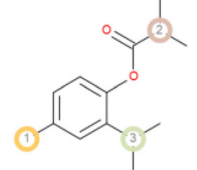
The Isothymol present score with -5.7853 Kcal/mol value and one hydrogen interaction with THR445 amino acids of 6vw1 target active site, the score β -D- Mannose (Co-crystallized ligand) is -5.4107 Kcal/mol, 5 interactions with GLU406, GLU406, GLN442, GLN442, LYS441 residues target active site, the Thymol has -4,7450 Kcal/mol, 2 interactions with GLU406 and THR445, the score values for the Limonene, P-Cymene and γ -Terpinene are respectively -4.4067, -4.3630, -4.2320 Kcal/mol and they have none interactions with residues target, Chloroquine has -6.4530 Kcal/mol score value, 2 interactions with OE1-GLU402 and OE1-GLU406 amino acids target and Captopril present -5.2248 Kcal/mol, one interaction with NZ-LYS 441 residues of 6vw1 target. We compared all the values score complexes; we found that complex formed by 6vw1-Isothymol has the lowest value energy and giving the best docking score compared to β -D- Mannose co-crystallized inhibitor and Captopril. On the other hand Isothymol has a lower molecular weight than Chloroquine and it gives almost the same values of the score (-5.7853 Kcal/mol and -6.4530 Kcal/mol respectively) therefore we can consider that the two complexes 6vw1-Isothymol and 6vw1-chloroquine are stables with higher binding affinity. According to these docking results we can classify Isothymol as the good inhibitor of the enzyme ACE2 compared to the all ligands studied.

3.2. In silico evaluation of druglikness, ADME/toxicity properties and PASS prediction

This test is performed to facilitate the creation of new drug molecules, the molecules of which must comply with the conditions of the following five Lipinski's rule: molecular weight: ≤ 500 , number of hydrogen bond donors: ≤ 5 , number of hydrogen bond acceptors: ≤ 10 , lipophilicity (expressed in LogP): ≤ 5 and molar refractivity from 40 to 130 (Lipinski et al., 2001). The results of this study are shown in the Table 4.

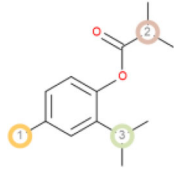
Chloroquine, Isothymol, β -D- Mannose, Captopril, Thymol, Limonene, P-Cymene and γ -Terpinene have respectively the following molecular weights: (319.87, 220.31, 180.16, 217.29, 150.22, 136.23, 134.22, 136.23) g/mol, they have all a molecular weight ≤ 500 g/mol, and also respectively present the following values of the topological polar surface (TPSA) (28.16, 26.30, 110.38, 96.41, 20.23, 0.00, 0.00, 0.00) Å². The lowest

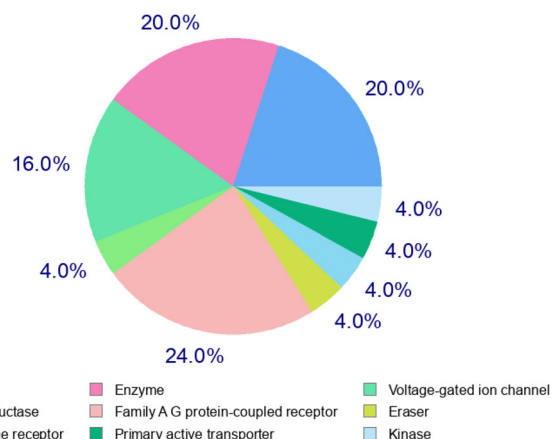
Table 8. List of the P450 sites of metabolism prediction study of the ligands molecules.

Drug Likeness Properties	Isothymol
1A2	
2A6	
2B6	
2C8	
2C9	
2C19	
2D6	
2E1	

(continued)

Table 8. Continued.

Drug Likeness Properties	Isothymol
3A4	

**Figure 6.** Top-25 of Target Predicted for Isothymol.

TPSA values always give good results, so we note that the molecules from the plant *Ammoides verticillata* are better behaved than the co-crystallized ligand and Captopril drug. By comparing the lipophilicity (LogP) values of our ligands series, we observe that they all have values less than 5 so they have shown very good results and can be easily absorbed in the body.

However, the LogS solubility values of the ligands tested are between -4.06 and 0.25. The Isothymol and chloroquine having the lowest values and β -D- Mannose having the greatest value, the lowest values of which are always appreciable. However all the ligands have a number of hydrogen bonding donors: ≤ 5 , a number of hydrogen bonding acceptors: ≤ 10 and also reactivity values between 35.75 and 130. So we can say that the five Lipinski's rule was verified for the ligands from the plant *Ammoides verticillata*. Veber's rule which represents the oral bioavailability of a possible drug molecule; it is verified for all the list of ligands studied.

We also note that another Egan's rule which defines the absorption of the drug molecule is verified for all ligands, on the other hand the 2 rules of Ghose's and Muegge's (Ghose et al., 1999; Veber et al., 2002; Egan et al., 2000; Muegge et al., 2001) are verified only for chloroquine drug and Isothymol therefore which means that Isothymol can be considered as a good drug. The ease of synthesizing a drug is given by the Synthetic Accessibility Score (SA). The molecule which gives a score 1 is easy to synthesize it, on the other hand the score 10 represents a difficulty of synthesis therefore according to our results the molecule Isothymol is easier

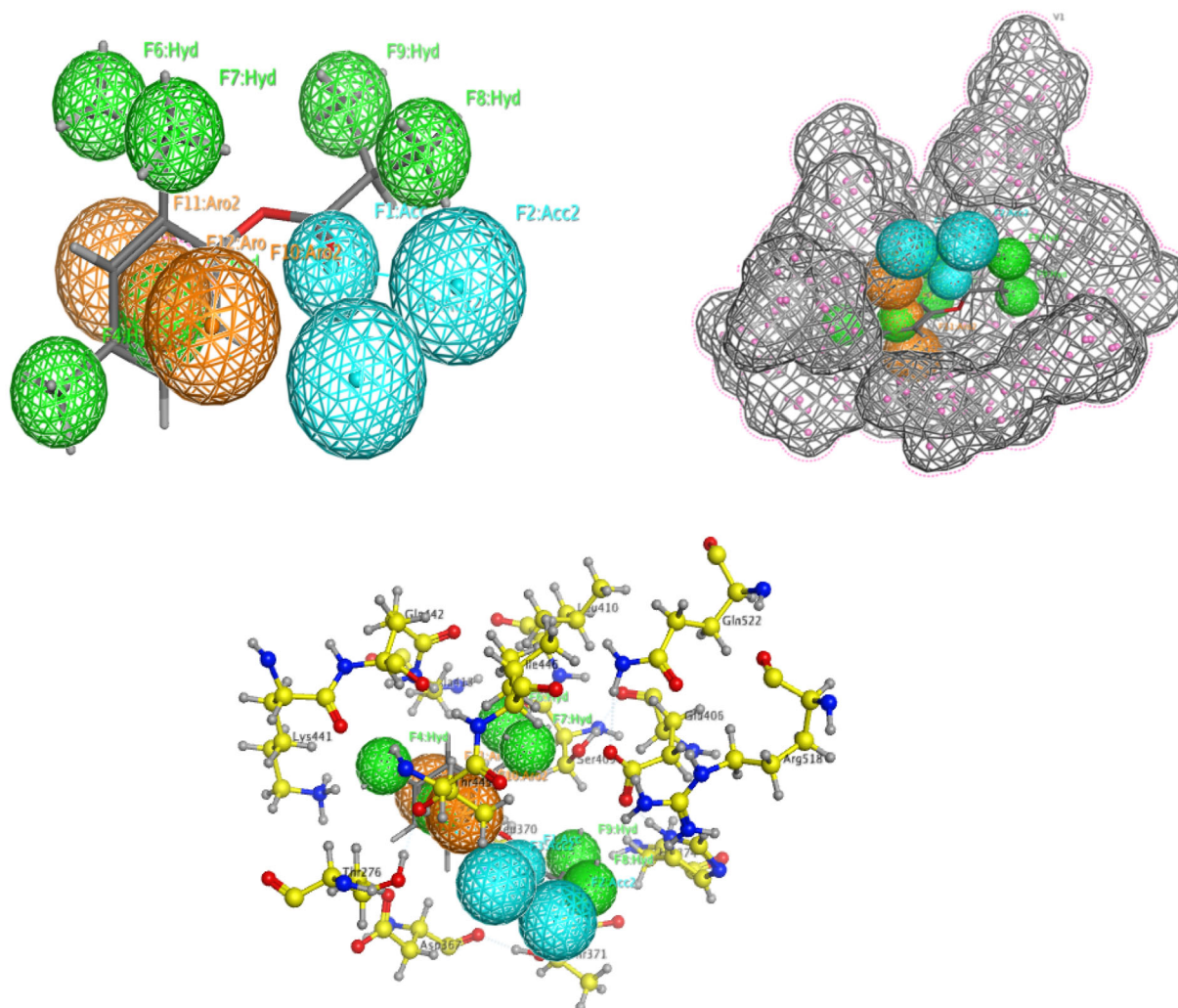


Figure 7. Pharmacophore Mapping of Isothymol. Here, cyan color- hydrogen bond acceptor, orange color-aromatic, green color-hydrophobic.

to synthesize it by contribution to the Chloroquine drug. We also notice that some ligands gives the reproductive effects, the irritant, Tumorigenic, Mutagenic properties and all the ligands from the plant *Ammoides verticillata* showed a bio-availability score of 0.55, and also good values of Druglikeness score, Solubility values and drug score. As conclusion the Isothymol which represents the highest yield in the plant *Ammoides verticillata* has followed the Lipinski's, Veber's, Egan's, Ghose's and Muegge's rules, it also has an 1.96 SA value so it is easy to synthesize it and it can to be considered as successful drug.

The results of the ADME tests are listed in the Table 5 these tests were carried out to determine the pharmacological and pharmacodynamic properties of a drug in the biological system.

In the Absorption part, Isothymol, Thymol, Limonene, P-Cymene, γ -Terpinene, Chloroquine and Captopril present at optimal Caco-2 permeability except β -D- Mannose at low Caco-2 permeability. This test is done to check whether the drug will be easily absorbed in the intestine or not. However Isothymol, Thymol, Limonene, P-Cymene, γ -Terpinene, Chloroquine and Captopril show a positive HIA test so they will be well absorbed by the human intestine. The inhibition

of the Pgp glycoprotein facilitates the transport of many drugs inside the cell, according to our results Isothymol is the only pgp inhibitor so it will be easily absorbed by the cells. Furthermore in the distribution part, the binding of drugs to plasma proteins is also an important pharmacological parameter; in our study the Captopril drug give a low capacity and negative test but Chloroquine drug and Isothymol show a good capacity and positive test for binding to plasma proteins so they are able to cross the blood-brain barrier. Also in the metabolism part, the cytochrome P450 is an enzyme family which metabolizes the drugs, so in our test only Isothymol is the inhibitor of CYP 450 A2, CYP4502C9, CYP4502C19, and also the substrate of CYP450A2, CYP4593A4, CYP4502C19, CYP4502D6, so the Isothymol can be metabolized by these enzymes . In the excretion part, the half-life of a drug describes the time required for the amount of a drug to be reduced in the body by half or 50% (Swierczewska et al., 2015; Smalling, 1996; Sahin & Benet, 2008). The series of ligands studied have a half-life between 1.129 h and 2.23 h of which the Isothymol ligand of the plant *Ammoides verticillata* has a significant half-life. That is to say, they give a potential effectiveness.

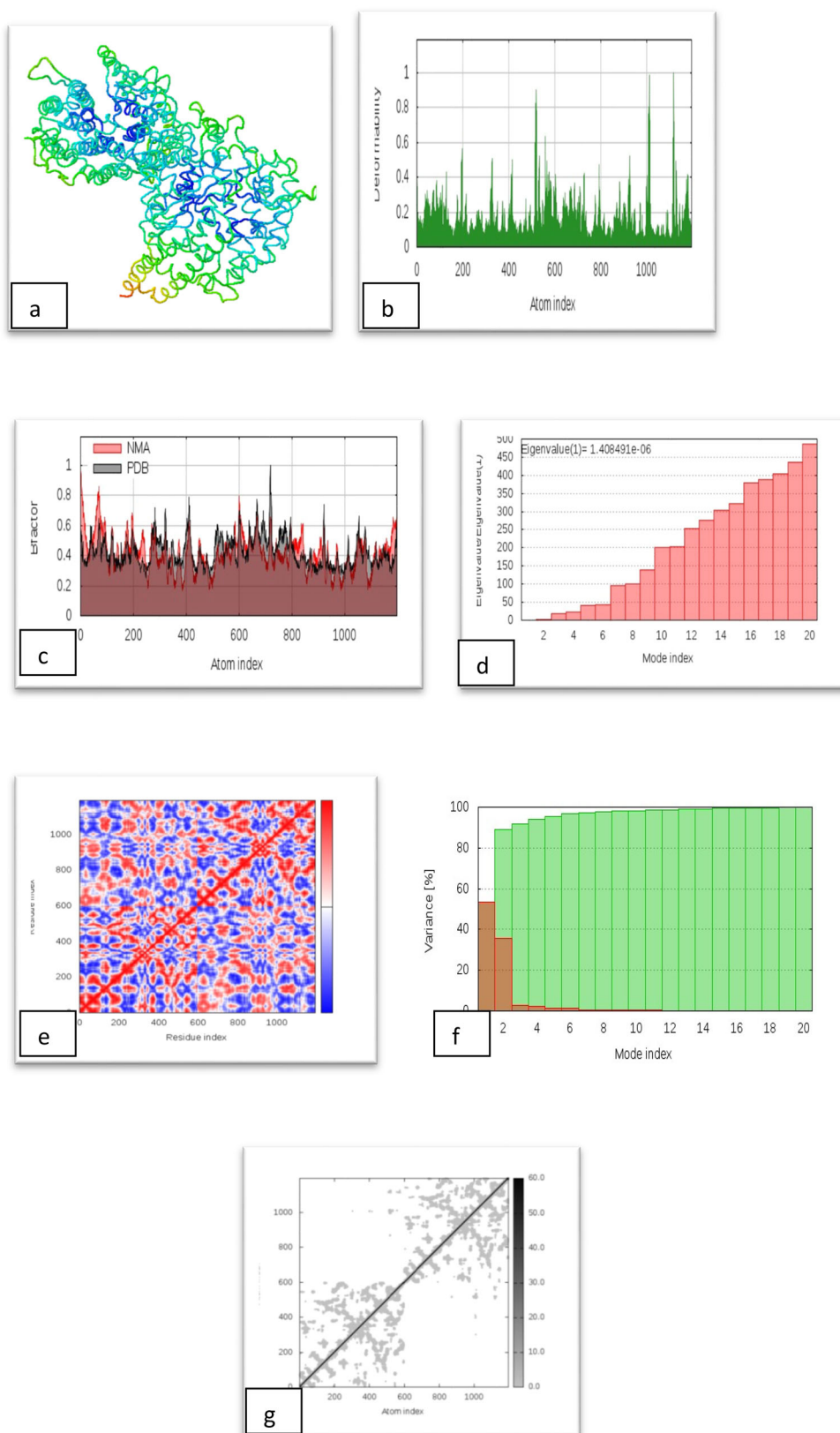


Figure 8. Results of molecular dynamics simulation of Isothymol-ACE2 Receptor. (a) NMA mobility, (b) deformability, (c) B-factor, (d) eigenvalues, (e) variance (red color indicates individual variances and green color indicates cumulative variances), (f) co-variance map (correlated (red), uncorrelated (white) or anti-correlated (blue) motions) and (g) elastic network (darker gray regions indicate more stiffer regions) of the complex.

Regarding the toxicity part, HERG is a K⁺ channel found in the heart muscle and ensures the correct rhythm of the heart, if HERG is blocked by certain drugs, it can cause

cardiac arrhythmia and death (Sanguinetti et al., 1995; Aronov, 2005), the Chloroquine drug which is used for the treatment of COVID-19 is blocker to HERG so it can cause

cardiac arrhythmia and death but the Isothymol is not HERG blocker which gives good result as drug. For the H-HT, AMES, Chloroquine drug gives the positive test but Isothymol present negative tests in the toxicity part, and all the molecules derived from the *Ammoides verticillata* present negative tests. In this ADMET part it can be suggested that the Isothymol molecule has better drug properties than the Chloroquine drug.

Prediction tests were also carried out for 10 biological activities, the results of which are in the Table 6. We note that all the ligands show some biological activities among the 10 tested.

Table 7 shows five toxic effects (Lagunin et al., 2000) tested for all the ligands of which it is noted that Chloroquine and captopril drugs presents the active Immunotoxicity test but Isothymol is inactive for the five toxic effects. However, according to Table 6, all the ligands Isothymol, Chloroquine and Captopril belong to toxicity class 4 with ($300 < LD50 \leq 2000$), so they would be harmful if swallowed.

The possible sites of metabolism by CYPs 1A2, 2A6, 2B6, 2C19, 2C8, 2C9, 2D6, 2E1 and 3A4 of Isothymol are illustrated in Table 8. The possible sites of a chemical compound, where the metabolism by the isoforms of CYP450 enzymes may be taken place, are indicated by circles on the chemical structure of the molecule (Zaretski et al., 2013). The P450 SOM predictions showed that Isothymol had 5 sites of metabolism (SOMs) for the CYP 450 2B6 enzyme, 4 sites for CYP 450 2A6, CYP 450 2C8, CYP 450 2D6, and 3 sites for CYP 450 1A2, CYP 450 2C9, CYP 450 2C19 and CYP 450 2E1 .

3.3. Target prediction

Molecular Target studies are important to find the phenotypical side effects or potential cross reactivity caused by the action of Isothymol the best ligand. The top 25 results are given in the Figure 6. The possible sites of target which the compound may bind to are mostly the targets of protease and oxidoreductase which stimulate the drug reaction accordingly.

3.4. Pharmacophore mapping

The Pharmacophore Mapping is carried for the Isothymol best ligand of the *Ammoides Verticilata*. Isothymol showed 2 hydrogen acceptor bonds, 6 Hydrophobic groups and 3 Aromatic rings. It also generated a good number of good contacts with the Pharmacophore of ACE2 Figure 7. The Pharmacophore of Isothymol generates a hypothesis which can be used successfully in biological screening for further experiments (Dixon et al., 2006).

3.5. Molecular dynamics simulation

The Molecular Dynamics Simulation results are showed in the Figure 8.

Figure 8a illustrates the normal mode analysis (NMA) of Isothymol-ACE2 complex. The deformability graph of the

complex illustrates the peak in the graphs correspond to the regions in the protein with deformability Figure 8b. The B-factor graph of the complex gives easy visualization and understanding of the comparison between the NMA and the PDB field of the complex Figure 8c. The eigenvalue of the complex is illustrated in Figure 8d. The docked complex generated eigenvalue of $1.408491e-06$. The variance graph indicates the individual variance by red colored bars and cumulative variance by green colored bars Figure 8e. Figure 8f illustrates the co-variance map of the complexes where the correlated motion between a pair of residues is indicated by red color, uncorrelated motion is indicated by white color and anti-correlated motion is indicated by blue color. The elastic map of the complex shows the connection between the atoms and darker gray regions indicate stiffer regions Figure 8g.

From the molecular dynamics study of Isothymol-ACE2 docked complex, it is clear that the complex had a very good amount of deformability Figure 8b as well as it had low eigenvalue of $1.408491e-06$, for this reason, this lower eigenvalue, represent the easier the deformability of the complex Figure 8d and also represents the motion stiffness of the protein complex.

However, the variance map showed high degree of cumulative variances than individual variances Figure 8e. The co-variance and elastic network map also produced satisfactory results Figure 8f and 8g.

In vivo studies have shown that the therapeutic qualities of *Ammoids verticillata* are known to be the oldest in local folk medicine. Indeed, Ibn El Beithar, in his treatise on the simple, in the article Athrilal indicates that this plant was used in the treatment of leprosy by a section of the tribe of Oudjeham, near Bougie in 1220 (Trabut, 1935b). It also has major antibacterial activity with a broad spectrum of action, antifungal (Dubey & Mishra, 1990; Grosjean, 2004), antiviral (Grosjean, 2004), it is used for the treatment of cholera (Avesina, 1985; Schirner, 2004), asthma (Avesina, 1985; Boskabady & Shaikhi, 2000; Schirner, 2004), fever, typhoid fever and bronchopulmonary diseases (Bekhechi, 2002). Thymol and Isothymol molecules from this plant are also widely used in cough medicine, throat irritation and cholera (Bhargava et al., 1961; Joshi et al., 1963).

In our study and after the best results obtained for the Isothymol ligand of *Ammoides verticilata* it can be used as potential agents to treat COVID-19 if we compared with Chloroquine and it emerged as the most potent anti-ACE2 agent.

4. Conclusion

The aim of our study is to investigate the potent of new natural's compounds such as Isothymol, Thymol, Limonene, P-Cymene and γ -Terpinene from *Ammoides verticillata* plant as inhibitors for ACE2 target. These compounds are tested *in silico* study for the inhibition to this enzyme. Molecular docking used to study interaction between new compounds and ACE2 with score energy investigation and druglikeness properties experiments, ADME/T tests, PASS prediction, the P450

Site of Metabolism (SOM), the Molecular Target, Pharmacophore Mapping, Molecular dynamics simulation have been performed to verify *in silico* the drug properties of the best ligand.

The top ligand Isothymol which is the major component (51.2%), in *Ammoides verticillata* has high binding affinity (Score) and one almost stable interaction with ACE2 target.

Our study showed for these natural components quite similar and very good results in all the aspects into account. Hence, Isothymol can be further developed as drug candidates against ACE2 receptor of coronaviruses, notably that responsible for severe acute respiratory syndrome. Finally we can suggest from this *in silico* study that *Ammoides verticillata* (Desf.) Briq. essential oils components can blocks the receptor ACE2 and could make it more difficult for coronavirus to enter cells, which could at least significantly slow the epidemic until the virus disappears. Though these properties are appreciable *in silico*, further studies of *in vitro* and clinical studies dealing with SARS-CoV-2 should be considered for further studies.

Disclosure statement

No potential conflict of interest was reported by the author(s).

References

- Aanouz, I., Belhassan, A., Khatabi, K. E., Lakhlifi, T., Idrissi, M. E., & Bouachrine, M. (2020). Moroccan Medicinal plants as inhibitors of COVID-19: Computational investigations. *Journal of Biomolecular Structure and Dynamics*. doi: [10.1080/07391102.2020.1758790](https://doi.org/10.1080/07391102.2020.1758790).
- Abdelouahid, D. E., & Bekhechi, C. (2002). Pouvoir antimicrobien de l'huile essentielle d'*Ammoides verticillata* (Nünkha). *Biologie et Santé*, 4, 91–100.
- Aronov, A. M. (2005). Predictive *in silico* modeling for hERG channel blockers. *Drug Discovery Today*, 10(2), 149–155. doi:[10.1016/S1359-6446\(04\)03278-7](https://doi.org/10.1016/S1359-6446(04)03278-7)
- Avesina, A. (1985). *Law in medicine* (2nd éd.). Soroush Press. pp 187.
- Awan, F., Obaid, A., Ikram, A., & Janjua, H. (2017). Mutation-structure-function relationship based integrated strategy reveals the potential impact of deleterious missense mutations in autophagy related proteins on hepatocellular carcinoma (HCC): A comprehensive informatics approach. *International Journal of Molecular Sciences*, 18(1), 139. doi: [10.3390/ijms18010139](https://doi.org/10.3390/ijms18010139)
- Bekhechi, C. (2002). Analyse de l'huile essentielle d'*Ammoides verticillata* (Nünkha) de la région de Tlemcen et étude de son pouvoir antimicrobien. *Mémoire de Magister*, option Biologie Moléculaire et Cellulaire, université Abou Bah Belkaid.
- Bekhechia, C., Brice Botib, J., Atik Bekkaraa, F., Eddine Abdelouahida, D., Casanovab, J., & Tomib, F. (2010). Isothymol in Ajowan essential oil. *Naturel Product Communication*, 5(7), 71107–71110.
- Bhargava, H. (1961). Anoxidative effect of Ajowan in a model system. *Journal of the American Oil Chemists' Society*, 72(10), 1215–1218. in Mehta, R. L., & Zayas, J. F. (1995). doi:[10.1007/BF02540992](https://doi.org/10.1007/BF02540992)
- Boopathy, S., Poma, A. B., & Kolandaivel, P. (2020). Novel 2019 coronavirus structure, mechanism of action, antiviral drug promises and rule out against its treatment. *Journal of Biomolecular Structure and Dynamics*. doi:[10.1080/07391102.2020.1758788](https://doi.org/10.1080/07391102.2020.1758788)
- Boskabady, M. H., & Shaikhi, J. (2000). Inhibitory effect of *Carum copticum* on histamine (H1) receptors of isolated guinea-pig. Tracheal chains. *Journal of Ethnopharmacology*, 69(3), 217–227. doi:[10.1016/S0378-8741\(99\)00116-6](https://doi.org/10.1016/S0378-8741(99)00116-6)
- Clément, G., & Slenzka, K. (Eds.). (2006). *Fundamentals of space biology: research on cells, animals, and plants in space*. Springer Science & Business Media. pp. 18.
- Daina, A., Michielin, O., & Zoete, V. (2017). SwissADME: A free web tool to evaluate pharmacokinetics, drug-likeness and medicinal chemistry friendliness of small molecules. *Scientific Reports*, 7(1), 42717. doi:[10.1038/srep42717](https://doi.org/10.1038/srep42717)
- Didierjean, C., & Tête-Favier, F. (2016). *Introduction to protein science. architecture, function and genomics*. 3rd ed. Arthur M. Lesk. Oxford University Press. pp. 466. Paperback. Price GBP 39.99. ISBN 9780198716846.
- Dixon, S. L., Smondjyev, A. M., Knoll, E. H., Rao, S. N., Shaw, D. E., & Friesner, R. A. (2006). PHASE: A new engine for pharmacophore perception, 3D QSAR model development, and 3D database screening: 1. Methodology and preliminary results. *Journal of Computer-Aided Molecular Design*, 20(10–11), 647–671. doi:[10.1007/s10822-006-9087-6](https://doi.org/10.1007/s10822-006-9087-6)
- Dubey, N. K., & Mishra, A. K. (1990). Evaluation of some essential oils against dermatophytes. *T Indian Drugs*, 27, 529–531.
- Egan, W. J., Merz, K. M., & Baldwin, J. J. (2000). Prediction of drug absorption using multivariate statistics. *Journal of Medicinal Chemistry*, 43(21), 3867–3877. doi:[10.1021/jm000292e](https://doi.org/10.1021/jm000292e)
- Elfiky, A. A., & Azzam, E. B. (2020). Novel Guanosine Derivatives against MERS CoVpolymerase: An *in silico* perspective. *Journal of Biomolecular Structure and Dynamics*. doi: [10.1080/07391102.2020.1758789](https://doi.org/10.1080/07391102.2020.1758789).
- Elmezayen, A. D., Al-Obaidi, A., Tegin Şahin, A., & Yelekçi, K. (2020). Drug repurposing for coronavirus (COVID-19): *in silico* screening of known drugs against coronavirus 3CL hydrolase and protease enzymes. *Journal of Biomolecular Structure and Dynamics*. doi: [10.1080/07391102.2020.1758791](https://doi.org/10.1080/07391102.2020.1758791)
- Enayatkhani, M., Hasaniazad, M., Faezi, S., Guklani, H., Davoodian, P., Ahmadi, N., Ali Einakian, M., Karmostaji, A., & Ahmadi, K. (2020). Reverse vaccinology approach to design a novel multi-epitope vaccine candidate against COVID-19: An *in silico* study. *Journal of Biomolecular Structure and Dynamics*. doi: [10.1080/07391102.2020.1756411](https://doi.org/10.1080/07391102.2020.1756411)
- Ghose, A. K., Viswanadhan, V. N., & Wendoloski, J. J. (1999). A knowledge-based approach in designing combinatorial or medicinal chemistry libraries for drug discovery. 1. A qualitative and quantitative characterization of known drug databases. *Journal of Combinatorial Chemistry*, 1(1), 55–68. doi:[10.1021/cc9800071](https://doi.org/10.1021/cc9800071)
- Grosjean, N. (2004). *Huiles essentielles: Se soigner par l'aromathérapie*. Ed. Eyrolles, pp 98.
- Guastalegname, M., & Vallone, A. (2020). Could chloroquine/hydroxychloroquine be harmful in Coronavirus Disease 2019 (COVID-19) treatment? *Clinical Infectious Diseases*, [Published online ahead of print, 2020 Mar 24]. doi:[10.1093/cid/ciaa321](https://doi.org/10.1093/cid/ciaa321)
- Gupta, M. K., Vemula, S., Donde, R., Gouda, G., Behera, L., & Vadde, R. (2020). *In-silico* approaches to detect inhibitors of the human severe acute respiratory syndrome coronavirus envelope protein ion channel. *Journal of Biomolecular Structure and Dynamics*. doi: [10.1080/07391102.2020.1751300](https://doi.org/10.1080/07391102.2020.1751300)
- Hasan, A., Ahamad Paray, B., Hussain, A., Ali Qadir, F., Attar, F., Mohammad Aziz, F., Sharifi, M., Derakhshankhah, H., Rasti, B., Mehrabi, M., Shahpasand, K., Akbar Saboury, A., & Falahati, M. (2020). A review on the cleavage priming of the spike protein on coronavirus by angiotensin-converting enzyme-2 and furin. *Journal of Biomolecular Structure and Dynamics*. doi: [10.1080/07391102.2020.1754293](https://doi.org/10.1080/07391102.2020.1754293)
- Higley, C., & Higley, A. (2005). *Quick reference guide for using essential oils*. 9th ed. Abundant Health. Orange, pp. 6–10.
- Hopkins, C. (2020). "Loss of sense of smell as marker of COVID-19 infection". Ear, Nose and Throat surgery body of United Kingdom. Retrieved 28 March 2020.
- Hui, D S., Azhar, I. E., Madani, T. A., Ntoumi, F., Kock, R., Dar, O., Ippolito, G., Mchugh, T. D., Memish, Z. A., Drosten, C., Zumla, A., & Petersen, E. (2020). The continuing 2019-nCoV epidemic threat of novel coronaviruses to global health—The latest 2019 novel coronavirus outbreak in Wuhan, China. *International Journal of Infectious Diseases*, 91, 264–266. doi:[10.1016/j.ijid.2020.01.009](https://doi.org/10.1016/j.ijid.2020.01.009)
- HyperChem v8. (2009). Molecular Modelling System, Hypercube Inc., 1115 NW 4th Street, Gainesville, FL 32601, USA.

- Jabeer Khan, R., Jha, R. K., Muluneh Amera, G., Jain, M., Singh, E., Pathak, A., Prabha Singh, R., Muthukumar, J., & Singh, A. K. (2020). Targeting SARS-CoV-2: A systematic drug repurposing approach to identify promising inhibitors against 3C-like proteinase and 2-O-ribose-methyltransferase. *Journal of Biomolecular Structure and Dynamics*, 20 April. doi: [10.1080/07391102.2020.1753577](https://doi.org/10.1080/07391102.2020.1753577)
- Joshi, B. S., Ramanujam, S., & Sahena, M. B. L. (1963). Improvement of some essential oil bearing spice plants. *Bull. Regional Res. Lab. Ja*, 1, 94–100.
- Kambouche, N., & El-Abed, D. (2003). Composition of the volatile oil from the aerial parts of *Trachyspermum ammi* (L.) Sprague from Oran (Algeria). *Journal of Essential Oil Research*, 15(1), 39–40. doi: [10.1080/10412905.2003.9712259](https://doi.org/10.1080/10412905.2003.9712259)
- Khan, S. A., Zia, K., Ashraf, S., Uddin, R., & Ul-Haq, Z. (2020). Identification of chymotrypsin-like protease inhibitors of SARS-CoV-2 via integrated computational approach. *Journal of Biomolecular Structure and Dynamics*. doi: [10.1080/07391102.2020.1751298](https://doi.org/10.1080/07391102.2020.1751298)
- Lagunin, A., Stepanchikova, A., Filimonov, D., & Poroikov, V. (2000). PASS: 2000. prediction of activity spectra for biologically active substances. *Bioinformatics*, 16(8), 747–748. doi: [10.1093/bioinformatics/16.8.747](https://doi.org/10.1093/bioinformatics/16.8.747)
- Lawrence, B. M. (2006). Progress in essential oils. *Perfumer & Flavorist*, 31, 63–64.
- Li, F., Li, W., Farzan, M., et., & Harrison, S. C. (2005). Structure of SARS Coronavirus spike receptor-binding domain complexed with receptor. *Science*, 309 (5742), 1864–1868. doi: [10.1126/science.1116480](https://doi.org/10.1126/science.1116480)
- Lipinski, C. A., Lombardo, F., Dominy, B. W., & Feeney, P. J. (2001). Experimental and computational approaches to estimate solubility and permeability in drug discovery and development settings. *Advanced Drug Delivery Reviews*, 46(1–3), 3–26. doi: [10.1016/j.addr.2012.09.019](https://doi.org/10.1016/j.addr.2012.09.019)
- López-Blanco, J. R., Aliaga, J. I., Quintana-Ortí, E. S., & Chacón, P. (2014). iMODS: Internal coordinates normal mode analysis server. *Nucleic Acids Research*, 42(W1), W271–276. doi: [10.1093/nar/gku339](https://doi.org/10.1093/nar/gku339)
- López-Blanco, J. R., Garzón, J. I., & Chacón, P. (2011). iMod: Multipurpose normal mode analysis in internal coordinates. *Bioinformatics*, 27(20), 2843–2850. doi: [10.1093/bioinformatics/btr497](https://doi.org/10.1093/bioinformatics/btr497)
- Molecular Operating Environment (MOE). (2013). Chemical Computing Group Inc., 1010 Sherbooke St. West, Suite #910, Montreal, QC, Canada, H3A 2R7, (2014).
- Muegge, I., Heald, S. L., & Brittelli, D. (2001). Simple selection criteria for drug-like chemical matter. *Journal of Medicinal Chemistry*, 44(12), 1841–1846. doi: [10.1021/jm015507e](https://doi.org/10.1021/jm015507e)
- Muralidharan, N., Sakthivel, R., Velmurugan, D., & Michael Gromiha, M. (2020). Computational studies of drug repurposing and synergism of lopinavir, oseltamivir and ritonavir binding with SARS-CoV-2 protease against COVID-19. *Journal of Biomolecular Structure and Dynamics*. doi: [10.1080/07391102.2020.1752802](https://doi.org/10.1080/07391102.2020.1752802)
- Narayana, C., Somayajulu, B. A. R., & Thirumala, S. D. (1967). Recovery of fatty oil from spent seeds of Ajowan. *Trachyspermum Ammi* Linn.). *Indian Journal of Technology*, 5, 268–269.
- Pant, S., Singh, M., Ravichandiran, V., Murty, U. S. N., & Srivastava, H. (2020). Peptide-like and small-molecule inhibitors against Covid-19. *Journal of Biomolecular Structure and Dynamics*. doi: [10.1080/07391102.1757510](https://doi.org/10.1080/07391102.1757510)
- Pole, S. (2013). *Ayurvedic medicine the principles of traditional practice*, edited by S. Dragon, pp. 122–123.
- Prabhakar, P. K., Srivastava, A., Rao, K. K., & Balaji, P. V. (2016). Monomerization alters the dynamics of the lid region in *Campylobacter jejuni* CstII: An MD simulation study. *Journal of Biomolecular Structure and Dynamics*, 34(4), 778–791. doi: [10.1080/07391102.2015.1054430](https://doi.org/10.1080/07391102.2015.1054430)
- Quezel, P., & Santa, S. (1963). *Nouvelle flore de l'Algérie et des régions désertiques méridionales*. Tome II. CNRS, pp. 671.
- Sahin, S., & Benet, L. Z. (2008). The operational multiple dosing half-life: A key to defining drug accumulation in patients and to designing extended release dosage forms. *Pharmaceutical Research*, 25(12), 2869–2877. doi: [10.1007/s11095-008-9787-9](https://doi.org/10.1007/s11095-008-9787-9)
- Sandberg, F., & Corrigan, D. (2001). *Natural remedies, their origins and uses*. Taylor & Francis.
- Sanguinetti, M. C., Jiang, C., Curran, M. E., & Keating, M. T. (1995). A mechanistic link between an inherited and an acquired cardiac arrhythmia: HERG encodes the IKr potassium channel. *Cell*, 81(2), 299–307. doi: [10.1016/0092-8674\(95\)90340-2](https://doi.org/10.1016/0092-8674(95)90340-2)
- Sarma, P., Sekhar, N., Prajapat, M., Avti, P., Kaur, H., Kumar, S., Singh, S., Kumar, H., Prakash, A., Prasad Dhibar, D., & Medhi, B. (2020). In-silico homology assisted identification of inhibitor of RNA binding against 2019-nCoV N-protein (N terminal domain). *Journal of Biomolecular Structure and Dynamics*. doi: [10.1080/07391102.2020.1753580](https://doi.org/10.1080/07391102.2020.1753580)
- Schirner, M. (2004). Huiles essentielles: Description de plus de 200 huiles essentielles et huiles végétales. *Guy Trédaniel*, 23.
- Shang, J., Ye, G., Shi, K., Wan, Y. S., Luo, C. M., Aihara, H., Geng, Q. B., Auerbach, A., & Li, F. (2020). National Institutes of Health/National Institute of General Medical Sciences (NIH/NIGMS).
- Simon, L., Imane, A., Srinivasan, K. K., Pathak, L., & Daoud, I. (2017). In silico drug-designing studies on flavanoids as anticancer agents: Pharmacophore mapping, molecular docking, and Monte Carlo method-based QSAR Modeling. *Interdisciplinary Sciences: Computational Life Sciences*, 9(3), 445–458. doi: [10.1007/s12539-016-0169-4](https://doi.org/10.1007/s12539-016-0169-4)
- Smalling, R. W. (1996). Molecular biology of plasminogen activators: What are the clinical implications of drug design? *The American Journal of Cardiology*, 78(12A), 2–7. doi: [10.1016/s0002-9149\(96\)00736-9](https://doi.org/10.1016/s0002-9149(96)00736-9)
- Stewart, J. J. (2007). Optimization of parameters for semiempirical methods V: Modification of NDDO approximations and application to 70 elements. *Journal of Molecular Modeling*, 13(12), 1173–1213. doi: [10.1007/s00894-007-0233-4](https://doi.org/10.1007/s00894-007-0233-4)
- Swierczewska, M., Lee, K. C., & Lee, S. (2015). What is the future of PEGylated therapies. *Expert Opinion on Emerging Drugs*, 20(4), 531–536. doi: [10.1517/14728214.2015.1113254](https://doi.org/10.1517/14728214.2015.1113254)
- Trabut, L. (1935a). Flore du Nord de l'Afrique: Répertoire des noms indigènes des plantes spontanées, cultivées et utilisées dans le Nord de l'Afrique. *Collection du Centenaire de l'Algérie*, Alger.
- Trabut, L. C. (1935b). Répertoire des noms indigènes des plantes spontanées, cultivées et utilisées dans le nord de l'Afrique. Alger. (Collection du centenaire de l'Algérie. Flore du nord de l'Afrique), 355.
- Veber, D. F., Johnson, S. R., Cheng, H. Y., Smith, B. R., Ward, K. W., & Kopple, K. D. (2002). Molecular properties that influence the oral bioavailability of drug candidates. *Journal of Medicinal Chemistry*, 45(12), 2615–2623. doi: [10.1021/jm020017n](https://doi.org/10.1021/jm020017n)
- Velavan, T. P., & Meyer, C. G. (2020). The COVID-19 epidemic. *Tropical Medicine & International Health*, 278–280.
- Zaretski, J., Bergeron, C., Huang, T-w., Rydberg, P., Swamidass, S. J., & Breneman, C. M. (2013). RS-WebPredictor: A server for predicting CYP-mediated sites of metabolism on drug-like molecules. *Bioinformatics*, 29(4), 497–498. doi: [10.1093/bioinformatics/bts705](https://doi.org/10.1093/bioinformatics/bts705)